The neural dynamics of positive and negative expectations of pain

Authors: Christoph A. Wittkamp[1], Maren-Isabel Wolf[1], Michael Rose*

Department of Systems Neuroscience, University Medical Center Hamburg-Eppendorf

[1] These authors contributed equally to this work.

*** Correspondence address:**

Department of Systems Neuroscience, University Medical Center Hamburg-Eppendorf

Martinistr. 52, Building W34

20248 Hamburg, Germany

Phone: +49-40-7410-54730, Fax: +49-40-7410-59955

Email: rose@uke.de

Abstract

Pain is heavily modulated by expectations. Whereas the integration of expectations with sensory information has been examined in some detail, little is known about how positive and negative expectations are generated and their neural dynamics from generation over anticipation to the integration with sensory information. The present preregistered study employed a novel paradigm to induce positive and negative expectations on a trial-by-trial basis and examined the neural mechanisms using combined EEG-fMRI measurements (n=50). We observed substantially different neural representations between the anticipatory and the actual pain period. In the anticipation phase i.e., before the nociceptive input, the insular cortex, dorsolateral prefrontal cortex (DLPFC), and anterior cingulate cortex (ACC) showed increased activity for directed expectations regardless of their valence. Interestingly, a differentiation between positive and negative expectations within the majority of areas only occurred after the arrival of nociceptive information. FMRI-informed EEG analyses could reliably track the temporal sequence of processing showing an early effect in the DLPFC, followed by the anterior insula and late effects in the ACC. The observed effects indicate the involvement of different expectation-related subprocesses, including the transformation of visual information into a value signal that is maintained and differentiated according to its valence only during stimulus processing.

1. Introduction

Nociceptive input can result in highly variable sensations of pain with expectations playing a crucial role in pain modulation (Atlas & Wager, 2012). Positive expectations can lead to hypoalgesia (placebo effect), while negative expectations can increase the perceived intensity of pain (nocebo effect; Kong & Benedetti, 2014). Although many studies have shown that expectations can influence pain perception, the neuronal processes underlying the generation of expectations prior to the appearance of the pain stimulus are not yet fully understood (Benedetti, 2014; Büchel et al., 2014; Koyama et al., 2005; Wager & Atlas, 2015). Several studies have demonstrated that placebo and nocebo effects influence brain activity during pain perception (Egorova et al., 2015; Wager & Atlas, 2015; Zunhammer et al., 2021). This may occur through multiple pathways that are involved in integrating expectations and sensory information (Geuter et al., 2017). Especially the descending pain modulatory system (DPMS; Geuter et al., 2017; Tu et al., 2022) is associated with placebo and nocebo effects and is thought to consist of areas like the periaqueductal grey (PAG), dorsolateral prefrontal cortex (DLPFC), anterior cingulate cortex (ACC), and amygdala (Eippert et al., 2009), as well as frontal areas like the vmPFC (Geuter et al., 2017; Tu et al., 2022). Further, placebo and nocebo effects modulate activity in areas classically associated with pain processing like the thalamus and the insula during noxious stimulation (Atlas & Wager, 2014; Wager & Atlas, 2015; Wager et al., 2004; Zunhammer et al., 2021).

A central feature of expectations is that they are generated prior to the appearance of the stimulus and should therefore be reflected in anticipatory neural activity (Kong et al., 2007; Wager et al., 2004). The mere expectation of the appearance of a painful stimulus has been shown to activate regions relevant to

subsequent pain processing, such as the insula, DLPFC, and thalamus (Palermo et al., 2015; Ploghaus et al., 1999). Similarly, there is evidence that expecting reduced pain (e.g. via a placebo) modulates activity in parts of the DPMS and the insula already during pain anticipation (Wager et al., 2011). This includes the DLPFC (Amanzio et al., 2013; Geuter et al., 2013; Wager et al., 2004; Watson et al., 2009) and the ACC (Amanzio et al., 2013; Geuter et al., 2013) and takes place prior to the widespread modulation of neural activity in the DPMS during pain processing (Amanzio et al., 2013; Atlas & Wager, 2014). The activation of brain areas prior to the administration of a painful stimulus aligns with the general framework of placebo effects and nocebo effects proposed by Büchel et al. (2014). This framework posits that placebo hypoalgesia and nocebo hyperalgesia can be attributed to predictive coding, suggesting that perception is the result of a constant matching of incoming sensory data with the top-down predictions of an internal or generative model (Büchel et al., 2014). The top-down predictions should be reflected in the expectation generation happening before the stimulus. However, the neural mechanisms of this process remain unclear, with little information about where and how the expectations relevant for these top-down predictions are generated. Further, it is uncertain whether the anticipatory modulation reported in the literature reflects only a pre-activation of later relevant networks or indicates functionally distinct processes in expectation generation. Comparing neural processing during both the anticipatory and pain periods prior to the stimulus is crucial for better dissociating the formation and maintenance of pain-related expectations from their integration with nociceptive input (Wager et al., 2004).

Another important factor when examining the representation of expectations is their valence, i.e. whether they are positive (as in placebo effects) or negative (as in nocebo effects). It remains elusive whether positive and negative expectations share

a common neural basis or depend on different networks (Freeman et al., 2015). On the basis of behavioral differences between positive and negative expectations, such as their varying correlations with the amount of prior experience and differences in learning (Colloca et al., 2010; Colloca et al., 2008), it seems reasonable to assume at least partially dissimilar neural representations of positive and negative expectations. Especially during pain perception, there is evidence of distinct neural processes for positive and negative expectations, as well as valence-dependent modulation of similar systems. More specifically, some findings suggest differential modulation of activity in key areas of the DPMS and reward system by the valence of expectations (Benedetti et al., 2020; Crawford et al., 2021; Koyama et al., 2005; Scott et al., 2008). Alternatively, some studies have reported the absence of shared brain activations during the perception of pain (Bingel et al., 2011; Freeman et al., 2015; Fu et al., 2021; Shi et al., 2021; Shih et al., 2019). Similar findings have been reported during pain anticipation, as some areas have been reported to be specifically activated for either placebo or nocebo (Fu et al., 2021; Rossettini et al., 2023) or show opposing valence-dependent responses (Amanzio et al., 2013; Kong et al., 2008; Palermo et al., 2015). However, there is conflicting evidence of shared anticipatory activation for both placebo and nocebo in some areas of the DPMS like the DLPFC and ACC (Amanzio et al., 2013; Amanzio & Palermo, 2019; Colloca & Benedetti, 2007; Frisaldi et al., 2015; Manaï et al., 2019; Palermo et al., 2015; Rossettini et al., 2023; Schmid et al., 2015). This illustrates an ongoing debate about whether there is a common neural basis of positive and negative expectations instead of entirely separated representations (Freeman et al., 2015; Fu et al., 2021). Taken together, the neuronal representations of positive and negative expectations may consist of shared valence-neutral processes (common effects) and different or differentially modulated valence-dependent processes (distinct effects), and this relationship may change over time from the

119 formation of expectations until their integration with the sensory information. To
120 adequately examine common and distinct neuronal representations, it is imperative to
121 compare positive and negative expectations against each other, as well as to an
122 appropriate control condition without any directed expectation, meaning that
123 perception is not biased into any direction in this condition. Hence, in this study, we
124 implemented a within-subjects design in which participants were subjected to positive,
125 negative, or neutral expectations on a trial-by-trial basis, enabling an exploration of
126 common and distinct processes.

127 Even during the anticipation phase, it is reasonable to presume the involvement
128 of distinct processes unfolding in a temporal sequence. For instance, the visual cue
129 must first be encoded and transformed into an expectation signal that can be
130 interpreted by a “pain system”. A potential candidate for this integration process is the
131 insula, which is recognized for its function as a multimodal network hub (Adler-Neal et
132 al., 2019; Dionisio et al., 2019; Lu et al., 2016). The multimodal role of the insula is
133 further reflected in its role in fear conditioning, with the insula being associated with
134 threat (Fullana et al., 2016), while other areas that are important for placebo
135 modulations like the vmPFC are closely connected to the default mode network,
136 potentially reflecting a safety signal (Fullana et al., 2016). Within the DPMS, prefrontal
137 areas have been suggested to provide predictions for downstream pain-sensitive
138 systems, implying an early role within this system (Geuter et al., 2017; Koban et al.,
139 2017; Wager & Atlas, 2015). Subsequently, it appears plausible that other areas of the
140 DPMS would need to be “informed” and activated in close temporal proximity to the
141 pain stimulus in order to exert their influence on pain perception (Amanzio et al., 2013).
142 The assessment of the temporal profile of expectancy generation is beyond the
143 possibility of fMRI. We therefore combined fMRI with simultaneous EEG

measurements, allowing us to temporally localize neural activity by utilizing the temporal and spatial advantages of both techniques at the single trial level.

In this study, we investigated the neural basis of the common and distinct processes underlying positive and negative expectations, and the formation and integration of expectations into pain perception, using a novel paradigm that allowed the manipulation of expectations on a trial-by-trial basis, while EEG and fMRI measures were recorded. We presented cues to induce expectations (positive, negative, or neutral expectations) followed by an anticipatory period in which different expectations emerged. This allowed us to examine the distinct and common effects of placebo and nocebo in the anticipation and pain phase by comparing the different expectation conditions. We focused on the evaluation of the different neuronal processes that contribute to the generation of directed expectations (i.e. positive and negative) in the anticipatory period and the effects during pain perception, using combined EEG and fMRI.

Based on the literature and the assumed theoretical approach of predictive coding, proposing an expectation formation before a stimulus, we expected that representations of pain-related expectations undergo dynamic changes during the anticipation phase and pain phase, reflecting different processes during these phases such as expectation formation, expectation integration, and pain modulation. These processes could involve either separate networks during the anticipation and pain phase or they could take place in the same networks, with the anticipatory activity having preparatory qualities for the later perception. Further, different patterns of activity for positive and negative expectations could arise. If the valences do not differ in their activation patterns either during pain anticipation or pain processing, this would mark similar processes for both positive and negative expectations. On the other hand,

169 different effects would either indicate distinct processes or a different modulation of the
170 same process. We would mainly expect a distinct nature of the valences, but that
171 similar areas would be engaged throughout anticipation and pain processing.
172 Therefore, we hypothesized to see neural representations of expectations in similar
173 areas during the anticipation and pain phase, albeit that positive and negative valences
174 would be differentially represented, marking dissociable dynamics of positive and
175 negative expectations.
176

177 **2. Results**

178 In total, we investigated 50 participants (32 female) in a combined EEG-fMRI
179 paradigm. In short, participants were told that they would be given real-time visual
180 feedback on their current pain sensitivity based on their EEG activity using a Brain-
181 Computer Interface (BCI). The feedback indicated one of three different brain states:
182 either a state of high pain sensitivity (red cue/nocebo condition/negative expectation),
183 low pain sensitivity (green cue/placebo condition/positive expectation), or that the BCI
184 algorithm would not make any prediction (yellow cue/control condition/neutral
185 expectation). In fact, the visual cues were not related to any brain activity but were only
186 used to produce the corresponding expectations. To reinforce expectations, we also
187 performed a learning (i.e. conditioning) phase. Here, red cues were paired with higher
188 pain intensity (VAS level 70), while green cues were paired with lower pain intensity
189 (VAS level 30). In the ensuing test phase (*see Figure 1*), temperatures were kept
190 constant (VAS level 60). Participants were informed that they would receive different
191 pain stimuli of medium intensity and were unaware that the stimulation temperature
192 was always exactly the same. In each trial, participants were given a BCI-based
193 feedback supposedly related to their current brain state (cue phase) and subsequently

194 rated their pain expectation for the next stimulus (expectation rating). After a fixed
195 anticipation phase, they were presented with a brief heat pain stimulus with a constant
196 target temperature irrespective of condition (pain phase), and lastly had to rate how
197 intense they perceived the stimulus (pain rating). Apart from EEG and fMRI we also
198 continuously recorded electrodermal activity.

199

200 *- Figure 1 -*

201

202 **2.1 Successful induction of placebo and nocebo effects in behavioral ratings and**
203 **skin conductance responses**

204 Our data show successfully induced expectations in line with the cued sham
205 brain states as evidenced by a significant main effect of condition in a repeated-
206 measures ANOVA for mean expectation ratings ($F_{(2,98)} = 86.51$, $p < .001$, $\eta_P^2 = .64$; *see*
207 *Figure 2A*). Expectation ratings were higher in the nocebo ($M = 65.80$, $SD = 15.80$)
208 compared to the control condition ($M = 48.58$, $SD = 13.79$, $p < .001$), which in turn
209 were higher than in the placebo condition ($M = 34.33$, $SD = 17.71$, $p < .001$). Similarly,
210 mean pain ratings were affected by our manipulation (rmANOVA: $F_{(2,98)} = 63.00$,
211 $p < .001$, $\eta_P^2 = .56$; *see Figure 2B*). Post-hoc Tukey tests revealed higher pain ratings
212 in the nocebo ($M = 56.80$, $SD = 14.21$) compared to the control condition ($M = 51.40$,
213 $SD = 14.31$, $p < .001$), which in turn led to higher pain ratings than the placebo
214 condition ($M = 44.88$, $SD = 15.06$, $p < .001$). Moreover, placebo (control - placebo) and
215 nocebo (nocebo - control) effects were significantly correlated across subjects for both
216 expectation ($r = 0.64$, $p < .001$) and pain ratings ($r = 0.30$, $p = .033$), indicating that
217 subjects who experienced stronger placebo effects also experienced larger nocebo
218 effects.

To assess whether ratings within the three conditions were stable or varied over time, we compared the relative variability index (Mestdagh et al., 2018), a measure that quantifies intra-subject variation over multiple ratings, between the three conditions and over the three measurement blocks. We observed differences in relative variance indices between conditions for both expectation $F(2,96) = 8.14$, $p < .001$) and pain ratings $F(2,96) = 3.41$, $p = .037$). For both measures, post-hoc tests revealed that there was significantly more variance in the placebo compared to the control condition (both $p_{holm} < .05$), but no difference between control and nocebo. Variance in expectation ratings decreased from the first block compared to the other two blocks ($F(1.35,64.64) = 5.69$, $p = .012$; both $p_{holm} < .05$), which was not the case for pain ratings. There was no interaction effect of block and condition for neither expectation ($F(2.65,127.06) = 0.40$, $p = .728$) nor pain ratings ($F(4,192) = 0.48$, $p = .748$), which implies that expectations were similarly dynamically updated in all conditions over the course of the experiment.

The expectation manipulation not only affected behavioral ratings but also the skin conductance responses (SCRs) to the pain stimuli (rmANOVA: $F(2,50) = 4.33$, $p = .018$, $\eta_P^2 = 0.15$; *see Figure 2C*). A posthoc Tukey test showed larger SCRs in the nocebo ($M = 0.05$, $SD = 0.09$) compared to the placebo condition ($M = -0.04$, $SD = 0.10$, $p = .049$). SCRs in the control condition ($M = -0.01$, $SD = 0.07$) did not significantly differ from neither nocebo ($p = .072$) nor placebo condition ($p = .607$).

- Figure 2 -

2.2 Successful induction of expectation effects in fMRI pattern

Induction of expectation effects was also tested in functional imaging data. For all fMRI analyses, a finite impulse response (FIR) model was used to characterize BOLD fluctuations over time from cue onset to the pain rating (*see Methods for details*). The stimulus intensity independent pain signature (SIIPS) has been introduced as a marker for subjective pain perception going beyond intensity differences as it has been reported to be affected by psychological factors such as expectations (Botvinik-Nezer et al., 2023; Woo et al., 2017). To further validate our experimental design, we estimated the SIIPS score for each condition during the pain phase as a marker for differences in pain perception between the three conditions (see Methods). A rmANOVA revealed significant differences between the three conditions within the pain period ($F(2,88) = 11.59$, $p < .001$, $\eta_P^2 = 0.21$), with Bonferroni-corrected paired *t*-tests showing significant differences between the placebo and nocebo condition ($t_{(44)} = 4.79$, $p < .001$) and between the nocebo condition and the control condition ($t_{(44)} = 3.36$, $p = .002$) but not between the control and the placebo condition ($t_{(44)} = 1.35$, $p = .184$, see *Figure 3*). We therefore conclude that the manipulation of expectations led to significant perceptual differences. Contrastingly, the SIIPS signature failed to discern between conditions during the anticipation period, suggesting fundamentally distinct processes in the two phases ($F(2,88) = 0.79$, $p = .455$, $\eta_P^2 = 0.02$).

- Figure 3 -

2.3 Neuronal representation of expectations over time

In our main analysis, we found a clear dissociation between the anticipation and pain phases with a predominantly common representation of positive and negative

expectations during the anticipation phase and a later shift towards distinct effects during the pain phase (*see Figure 4A*). In order to investigate how the representations of directed expectations changed over time from the anticipation to the pain phase, we identified common (i.e., positive and negative vs. control; constrained to areas with no statistical difference between positive and negative) and distinct (positive vs. negative) effects of directed expectations in each phase (*see Supplementary Tables 1-4 for all comparisons*). During the anticipation phase, common effects of directed expectations were found in several important areas of the DPMS e.g. in the bilateral DLPFC, bilateral ACC and right vmPFC, indicating that directed expectations were represented in a rather general and nonspecific way during this period. With the stimulus onset, activity in these areas showed differential activation between positive and negative expectations. Further differential activity was observed in e.g. left insula, amygdala, thalamus, and hippocampus during the pain phase.

Crucially, the bilateral DLPFC, right vmPFC, left anterior insula, and thalamus were engaged during both the anticipation and pain phases (*see Figure 4B*). In all these areas, directed expectations shifted from a common (positive and negative > control) towards a distinct representation (positive > negative: bilateral DLPFC, right vmPFC, and left anterior insula; negative > positive: thalamus) over time. In addition to these areas that are frequently related to expectation effects, the right angular gyrus was also engaged throughout the time course, similarly initially showing a common representation of positive and negative expectations during the anticipation phase and differentiating only during pain perception ($p < .05$ whole-brain FWE-corrected; *see Figure 5*).

The differences between the anticipation and the pain phase demonstrate that specific expectations were mediated by different processes during these phases and

292 arise from a dynamic interplay of brain regions such as the DLPFC, vmPFC, anterior
293 insula, and thalamus over time.
294
295 *- Figure 4 -*
296
297 *- Figure 5 -*
298
299 **2.4 Timing of effects during the anticipation phase**

300 To obtain detailed information on the temporal characteristics of the expectation
301 effects during pain anticipation, we performed fMRI-informed EEG analyses.
302 Specifically, we were interested in the temporal sequence of the areas involved. Single-
303 trial estimates of fMRI activity during the anticipation phase were correlated with time-
304 frequency decomposed EEG measures for each participant and then statistically
305 tested at the group level. This analysis was conducted separately for the identified
306 regions of interest that represented directed expectations during both the anticipation
307 and pain phase (left anterior insula, right vmPFC, bilateral DLPFC, and thalamus). We
308 further included the bilateral ACC, as we were interested in all areas that reflected
309 directed expectations during the anticipation phase.

310 Clear temporal differences between areas were observed. The earliest
311 correlation of fMRI activity with EEG oscillatory power was found in the left DLPFC
312 already during the expectation rating at theta to low gamma frequencies in a negative
313 direction (-6.3 until -4.4 s, 4 to 45.28 Hz; p = .007; see *Figure 6A*; additional information
314 for all regions can be found in *Supplementary Table 5*). Next, anticipatory activity in
315 the left anterior insula was associated with decreased EEG oscillatory power during
316 the late expectation rating and anticipation phase (-4.4 to -2.5 s) spanning from theta

317 to low gamma frequencies (5.67 to 32 Hz; $p < .001$; see *Figure 6B*). Lastly, we found
318 a significant positive association of EEG activity with fMRI activity in the right ACC
319 during the anticipation and early pain phase in the gamma frequency range (-3 to 0.3 s,
320 26.89 to 128 Hz; $p = .003$; see *Figure 6C*). As expected due to the close spatial
321 proximity, activity in the left ACC was similarly positively correlated with EEG activity
322 in the anticipation and pain phase (cluster 1: -2.3 to -1.3 s, 32 to 128 Hz; $p = .019$;
323 cluster 2: -0.9 to 0.3 s, 32 to 128 Hz; $p = .021$). We did not observe significant
324 correlations of EEG power with fMRI activity in the other ROIs.

325 In summary, the analyses indicated that areas exhibiting similar fMRI effects for
326 positive and negative expectations during the anticipation phase are linked to distinct
327 temporal and oscillatory patterns. Notably, the left DLPFC and the left anterior insula
328 displayed an early negative correlation between anticipatory activity and EEG power,
329 primarily in the lower frequency range. Conversely, the subsequent effects in the
330 bilateral ACC were associated with an increase in gamma oscillations and were
331 observed at later time points during the anticipation phase indicating different
332 processes.

333

334 *- Figure 6 -*

335

336 **3. Discussion**

337 The manipulation of positive, negative, or neutral expectations on a trial-by-trial
338 basis allowed for a detailed analysis of their neural representations during the
339 generation and integration of expectations with the nociceptive input. Our results
340 revealed fundamental differences between the anticipation and pain phase, indicating

341 the involvement of divergent processes. During the anticipation phase, valence-neutral
342 representations were observed in areas of the DPMS and the anterior insula. After the
343 onset of the nociceptive stimulus these areas showed differentiated representations
344 indicating separate processes for the formation of expectations and their integration
345 within stimulus processing. The excellent temporal resolution of our fMRI-informed
346 EEG measures further revealed a temporal sequence of expectation processing during
347 the anticipation phase, with an early effect within the DLPFC, followed by activation in
348 the anterior insula, and late effects within the ACC, in line with the occurrence of
349 different time-sensitive sub-processes of expectation generation in this phase.

350 Our novel within-subjects paradigm was highly effective, as expressed by 47
351 out of 50 subjects consistently expecting and perceiving the intensity of pain stimuli in
352 line with the cues that induced positive, negative or neutral expectations. The trial-by-
353 trial manipulation of expectations did not only affect self-reports, but also objective
354 markers such as skin conductance responses and scores of the SIIPS (Woo et al.,
355 2017). The SIIPS is an indicator of neural activity that tracks differences in pain
356 perception that go beyond pain intensity and is classically affected by placebo and
357 nocebo interventions (Botvinik-Nezer et al., 2023; Woo et al., 2017), thus serving as
358 an excellent manipulation check for our paradigm. In line with our expectations, the
359 SIIPS scores discriminated between positive and negative expectations only during
360 the pain phase and not during the anticipation phase. This is a first hint at substantially
361 different processes during the two phases.

362 The neural representations of directed expectations differed depending on the
363 valence of the expectation, i.e. if they were positive or negative and the time period. A
364 shift from common (valence-neutral) to distinct (valence-dependent) effects was
365 evident in areas classically involved in placebo analgesia during pain processing,

366 including the bilateral DLPFC, right vmPFC, left anterior insula, and thalamus. The
367 observation of this pattern in key areas of the DPMS indicates that the activation during
368 the anticipation phase is not just mere pre-activation for later pain modulation, but that
369 preparatory processes that are distinguishable from those that occur during pain
370 perception take place. These anticipatory processes may include expectation
371 generation and maintenance, while the focus shifts towards the integration of these
372 expectations into the sensory stream and the evaluation of the percept during pain
373 processing. Importantly, the spatial resolution of fMRI is limited when it comes to
374 discriminating whether the same pattern of activity is due to identical activation or to
375 activation in different sub-circuits within the same area. Nonetheless, the overlap of
376 areas is an indicator for similar processes involved in a more general preparation
377 process. The observed differentiation during pain is in agreement with the few studies
378 that looked into the neuronal representations of positive and negative expectations and
379 mainly found differential effects, e.g. opposite responses or differentially modulated
380 areas during pain (Benedetti et al., 2020; Crawford et al., 2021; Koyama et al., 2005;
381 Scott et al., 2008).

382 The network of the DPMS around the DLPFC, ACC and vmPFC appears to play
383 a pivotal role in expectation processes and in the valence-dependent modulation of
384 pain perception. Following the framework of predictive coding, our results would
385 suggest that the DPMS is the network responsible for integrating ascending signals
386 with descending signals in the pain domain and that this process is similar for positive
387 and negative valences during anticipation of pain but differentiates during pain
388 processing. One important node of the DPMS is the DLPFC. The outstanding role of
389 the DLPFC in placebo effects is well-established and supported by numerous reports
390 of increased DLPFC activity during pain anticipation (Watson et al., 2009) as well as
391 during pain processing (Zunhammer et al., 2021). This area has been classically

392 associated with top-down-regulation and expectation modulation (Geuter et al., 2017),
393 as when its neuronal excitability is experimentally manipulated, placebo effects can be
394 diminished or enhanced (Egorova et al., 2015; Krummenacher et al., 2010; Tu et al.,
395 2021). The early onset of DLPFC activity implied by the EEG analysis now suggests
396 that the DLPFC plays an important role in the initiation of both positive and negative
397 expectation effects within the DPMS prior to the noxious stimulation (Frisaldi et al.,
398 2015; Geuter et al., 2017; Rossettini et al., 2023; Wager & Atlas, 2015; Wager et al.,
399 2011). The vmPFC is another important hub within the DPMS which is suggested to
400 integrate the input from the DLPFC and to generate affective meaning in order to
401 maintain expectations (Geuter et al., 2017). It further modulates pain perception by
402 directly affecting brainstem systems (Koban et al., 2017), e.g. by influencing PAG
403 activity (Geuter et al., 2017). The notion that prefrontal areas exert top-down control
404 over other areas of the DPMS is further supported by the earlier timing of DLPFC
405 effects compared to the ACC (Craggs et al., 2014; Watson et al., 2009). The ACC also
406 has a direct influence on the activity of the PAG, suggesting that the ACC is another
407 crucial area for pain modulation (Geuter et al., 2017; Livrizzi et al., 2022). The effect of
408 the bilateral ACC at the transition from the anticipation to the pain phase as indicated
409 by our combined EEG-fMRI analysis could be interpreted as a preparatory mechanism
410 for the modulation of incoming sensory information in downstream areas, consistent
411 with its supposed role in the DPMS (Geuter et al., 2013; Geuter et al., 2017; Kong et
412 al., 2008). Using this framework, reports of ACC activations for both positive and
413 negative expectations during pain anticipation could be understood as a pre-activation
414 of the ACC for pain modulation in either direction (Rossettini et al., 2023). The link
415 between anticipatory activity in the ACC and EEG oscillatory activity was observed in
416 the high gamma band, which is consistent with findings that demonstrate a connection
417 between increased fMRI BOLD signals and a relative shift from lower to higher

frequencies (Kilner et al., 2005). Gamma oscillations have been repeatedly reported in the context of pain and expectations and have been interpreted as reflecting feedforward signals of noxious information (e.g.: Ploner et al., 2017; Strube et al., 2021). In combination with our findings, this might imply that high frequency oscillations may not only signal higher actual or perceived pain intensity during pain processing (Nickel et al., 2022; Ploner et al., 2017; Strube et al., 2021; Tu et al., 2016), but might also be instrumental in the transfer of directed expectations from anticipation into pain processing.

Similarly, a shift from valence-neutral towards valence-dependent processing over time was demonstrated in the anterior insula. The insula is a key brain region involved in the network responsible for pain processing (e.g., Atlas & Wager, 2014; Kober et al., 2008) but is also part of several non-pain-related networks and works as multimodal network hub (Horing & Büchel, 2022). Results of the fMRI-informed EEG analysis indicated early effects in the anticipatory period consistent with an early role of the anterior insula in expectation generation and initiation. Due to the multimodal nature of the insula, it may be speculated that multiple networks interact to integrate relevant information from different domains (e.g. from the visual cue and interoceptive information) into an expectancy signal in the anterior insula. Due to its connections and function within the salience network, this may involve encoding the expected threat level and salience of subsequent pain stimuli, leading to an anticipatory activation prior to the actual perceptual modulation (Taesler & Rose, 2016; Wiech et al., 2010). During pain perception, the anterior insula may then be more engaged in a network responsible for stimulus processing and evaluating actual salience and prediction errors in this perceptual process (Horing & Büchel, 2022), which may imply that the insula is involved in multiple tasks over time.

Similar to the anterior insula, the activation of the angular gyrus during pain processing and pain anticipation could be understood as an indicator for processes related to the formation and integration of directed expectations. The angular gyrus has been connected to expectation-related pain modulation only few times (e.g., Atlas & Wager, 2014; Tu et al., 2019) but its involvement is prominent in our results. Based on its presumed function in maintaining recollected multimodal representations (Jablonowski & Rose, 2022; Vilberg & Rugg, 2012), the angular gyrus may be engaged in transforming sensory information from the visual cues into expectancy signals that can be processed by e.g. the DPMS and salience network.

With our rather unconventional and new paradigm, we were able to manipulate participants expectations on a trial-by-trial level and derive insights on the neural dynamics of positive and negative expectations. While this may give rise to questions regarding the comparability of our study to previous paradigms and the manner in which our control condition was employed, we would argue that our expectation manipulation falls in line with a manipulation of treatment expectancies, a typical method of expectation manipulation in placebo paradigms (see Atlas & Wager, 2014). Accordingly, it is comparable to previous studies on placebo and nocebo effects. In our study, participants were presented with a cue that induced expectations regarding a ”treatment”, although in this case the “treatment” originated from changes in their own brain activity. This is, in a broader sense, comparable to studies utilizing sham TENS-devices that are supposedly altering peripheral pain transmission (Skvortsova et al., 2020).

Moreover, implementing a proper control condition in expectation modulation paradigms is an inherently difficult task as forming expectations about our environment is a natural process. Therefore, we recognize that participants most likely did form

468 expectations of medium pain intensities in the control condition over the course of the
469 experiment. This is in line with previous research on placebo and nocebo effects, in
470 which participants also typically rated control stimuli in between placebo and nocebo
471 conditions (Bingel et al., 2011; Colloca et al., 2010; Shih et al., 2019). However, we
472 would still argue that we can meaningfully compare the placebo and nocebo condition
473 to the control condition to investigate the neuronal underpinnings of expectation
474 effects. Independently of whether participants build up an expectation of "medium"
475 intensities in the control condition, which caused them to perceive stimuli in line with
476 this, or if they simply perceived the stimuli as they were (of medium intensity) with
477 limited effects of expectations, the crucial difference to the placebo and nocebo
478 conditions is that there was no alteration of perception due to previous experiences or
479 verbal information and no shift of perception from the actual stimulus intensity towards
480 any direction in the control condition. Thus, we were able to identify effects of directed
481 expectations by comparing positive and negative expectations to neutral expectations
482 as a baseline. Our analysis of within-condition variability further showed that ratings
483 indeed varied within conditions and that the amount of variation was comparable
484 between nocebo and control. Over time, expectations were dynamically updated in all
485 three conditions, speaking against alternative explanations of the rating differences
486 between conditions such as a regression to the mean of ratings in the control condition.

487 Based on the present results, understanding the processing of expectations
488 requires an examination of its temporal and spatial dynamics from anticipation to pain
489 processing, while comparing positive and negative valences to each other and to a
490 control condition. We found largely comparable activation for positive and negative
491 expectations during the anticipation phase, including regions outside of those
492 classically observed in pain processing and modulation. Based on the observed
493 temporal profiles, the DLPFC and anterior insula may be related to the top-down

494 initiation and generation of expectations, while the ACC is activated in close proximity
495 to pain onset as a direct link to pain modulation. During the pain phase, the focus shifts
496 from expectation generation and maintenance towards pain modulation in either
497 positive or negative direction, leading to distinct effects of positive and negative
498 expectations in many areas that initially encoded expectations independently of their
499 valence. It is not surprising that expectations are not a static process but involve
500 different time-dependent components, as pain perception was also recently described
501 as a complex process of interactions among multiple brain systems that are
502 reconfigured over time (Lee et al., 2022). Expectation generation, integration and pain
503 perception all appear to be dynamic processes, with both common and distinct routes
504 for positive and negative expectations, depending on the time point of examination.

505

506 **4. Methods**

507 **4.1. Participants**

508 In total, 55 volunteers were recruited via an online job platform and participated
509 in our preregistered study (German Clinical Trials Register; ID: DRKS00025872). All
510 participants were right-handed, had normal or corrected-to-normal vision, reported no
511 neurological or psychiatric diseases, pain conditions, current medication, substance
512 abuse, or pregnancy, and were non-smokers. They gave written informed consent and
513 were compensated with 15 Euros per hour of participation. Of these 55 participants, 5
514 had to be excluded from all analyses (4 due to technical issues leading to the abortion
515 of the measurement, 1 due to a severe BDI score), leading to a final sample size of
516 N = 50 (*see Table 1*). As preregistered, three participants who rated expectation and
517 pain averaged over the entire experiment higher for placebo compared to nocebo
518 and/or stated that they did not believe in the BCI method were excluded for the analysis

of neural data, as we reasoned that the analysis of expectation-related neural activity requires a successful induction of expectations. Analyses for fMRI data were performed additionally excluding 2 participants with bad MRI data (leading to *N* = 45 for fMRI analyses), and for combined EEG-fMRI analyses additionally excluding 4 participants with excessive artifacts and/or recording equipment malfunction (leading to *N* = 41 for combined EEG-fMRI analyses). The study was approved by the local ethics committee (PV7170).

- Table 1 -

4.2. Procedure

Pre-Measurements (Collaborative Research Centre recordings)

One day before the actual study, we recorded fMRI data (T1, functional EPI, DW EPI) and asked the participants to complete a comprehensive psychosocial questionnaire battery that will be analyzed by other projects under the structure of the overarching collaborative research center and are beyond the scope of this manuscript. Participants were pseudonymized using ALIIAS (Englert et al., 2023).

Main Experiment

The experiment consisted of four phases: a verbal instruction phase, a pain calibration phase, a conditioning phase, and a test phase. The experiment was programmed using Psychtoolbox3 (http://psychtoolbox.org/) for Matlab (Version R2021b; The MathWorks). Rating responses were given by the participants using a Button Box MR. Instructions and ratings were presented on an MR-compatible monitor with a resolution of 3840 x 2160, placed at one end of the scanner. Participants saw

the monitor through a mirror that was placed approximately 12 cm away from the participant's eyes and had a distance of approximately 151 cm from the monitor. Two researchers and one radiographer guided the participants through the instructions and preparations.

Verbal Instruction Phase

After being prepared for the EEG and fMRI recording, participants were verbally informed that their current oscillatory state of the primary somatosensory cortex would be measured in real-time using a BCI (Brain Computer Interface) and that this state would reflect their pain sensitivity. They were further told that the measured brain state would be visualized in the form of visual stimuli consisting of a brain image with the right primary somatosensory cortex highlighted in one of three different colors (green, red, or yellow). A green stimulus represented a state in which their brain would be less susceptible to pain, a red stimulus represented a state in which their brain would be highly susceptible to pain, and a yellow stimulus represented a state in which the algorithm was not able to detect a clear-cut state and would thus make no prediction (e.g. due to high fluctuations in brain activity or intermediate activity levels). With this procedure, a positive expectation was induced by the green cue, and a negative expectation was induced by the red cue. After the verbal instructions, participants were asked to fill out state questionnaires, including the State-Trait Anxiety Depression Inventory (Laux et al., 2013) and the Fear of Pain Questionnaire (McNeil & Rainwater, 1998).

Pain Calibration Phase

Heat stimuli were delivered with a PATHWAY CHEPS (Contact Heat-Evoked Potential Simulator) thermode (https://www.medoc-web.com/pathway-model-cheps),

570 which has a rapid heating rate of 70°C/s and a cooling rate of 40°C/s and can deliver
571 pain stimuli in the range of 30°C to 55°C in less than 300 ms. For all phases, the
572 baseline temperature was set to 32°C, and the rise and fall rate were set to 70°C/s.
573 The thermode head was attached to a location directly proximal to the volar mid-
574 forearm. Using a stepwise procedure, we determined individual temperatures for each
575 participant corresponding to values of VAS30, VAS60, and VAS70 on a visual analog
576 scale (VAS) from 0 ("no pain") to 100 ("unbearable pain"). Target temperatures were
577 calculated using linear regression.
578
579 ***Conditioning phase***
580 For the conditioning phase, the location of the thermode head was changed to
581 a location directly distal to the volar mid-forearm to avoid unnecessary sensitization of
582 one location and skin irritations. Participants were instructed that the next phase would
583 serve as the calibration of the BCI algorithm introduced in the verbal instruction phase.
584 They were informed that in this phase only green and red cues would appear because
585 the pain stimulation would only occur once a clear-cut state of their brain has been
586 detected. Each trial began with the presentation of either a red or green visual cue for
587 2 s, then the painful stimulus was administered for 4 s, and lastly, participants were
588 asked to rate their pain experience for 8 s. Between trials, there was a fully randomized
589 inter-trial interval (ITI) of between 2 and 7 s. During the painful stimulation and ITIs, a
590 fixation cross was presented in the middle of the screen. Perceived pain intensity was
591 again rated on a VAS from 0 ("no pain") to 100 ("unbearable pain"). Unbeknownst to
592 the participants, green cues were always followed by less painful stimuli (VAS30), and
593 red cues were always followed by more painful stimuli (VAS70). They received 10
594 stimuli of each condition, leading to 20 trials in total. The order of stimuli was pseudo-

randomized with the restrictions of no more than two direct repetitions of the same condition and the last two trials of this phase belonged to the less painful condition.

Test phase

For the test phase, the thermode head was once again attached to the location directly proximal to the volar mid-forearm. Participants were informed that the BCI algorithm has now been calibrated and would be tested in the next phase. They were told that the painful stimulation would occur at random predetermined points in time, so that either highly pain-sensitive (red; nocebo condition) or less pain-sensitive states (green; placebo condition) could be detected and reported back to the participant, or that they would receive feedback that the algorithm was not able to detect a clear-cut state (yellow; control condition). The trial structure was similar to the conditioning phase, with the change that after cue presentation, participants were asked to rate how painful they expect the next stimulus to be on a VAS ranging from 0 to 100 while the cue was still presented on the screen (4 s). After this expectation rating, a fixation cross was presented for 3.3 s (anticipation phase) before the pain stimulus was administered for 4 s (pain phase). Independently of the cue color, participants always received painful stimuli corresponding to values calibrated to VAS60. Importantly, participants were only informed that they would receive different stimuli of medium intensity and were thus not aware that the stimulation temperature remained constant. There were 30 cues of each condition followed by pain stimulation divided into three blocks, summing up to a total of 90 stimuli. Similarly to the conditioning phase, the ITI was fully randomized between 2 and 7 s. The order of cues was pseudo-randomized with no more than two direct repetitions of the same condition. Before each block, we applied one pain stimulus of VAS60 without a cue to desensitize the new skin area.

621 ***Follow-Up***

622 One week after the main experiment, participants were invited for a follow-up
623 measurement which is beyond the scope of this manuscript. They were asked to fill
624 out questionnaires, including the Beck Depression Inventory-II (Beck et al., 1996;
625 Hautzinger et al., 2006). Lastly, participants were debriefed and paid.

626

627 **4.3. Data acquisition**

628 **Electrodermal Data**

629 Electrodermal activity was measured with MRI-compatible electrodes on the
630 thenar and hypothenar. Electrodes were connected to Lead108 carbon leads (BIOPAC
631 Systems, Goleta, CA). The signal was amplified with an MP150 analogue amplifier
632 (also BIOPAC Systems) and sampled at 5,000 Hz using a CED 1401 analogue-digital
633 converter (Cambridge Electronic Design, Cambridge, UK).

634

635 **fMRI Data**

636 MRI was performed with a 3T Siemens PRISMA Scanner, and a 64-channel
637 head coil was used. On the day of the pre-measurements, a T1 image with the
638 following parameters was acquired: T1 FLASH 3D: TE 2.98 ms, TR: 2300 ms, matrix
639 flip angle: 9°, FOV 25.6 * 25.6 cm, TA: 7:22 min. Two sequences on the day of the
640 main experiment were acquired: An EPI BOLD sequence and a field map sequence.
641 Participants were prepared with a 64-channel standard BrainCap MR for 3 Tesla (2020
642 Version) and the EPI BOLD sequence had therefore to be adjusted to meet the
643 necessary safety criteria. The following parameters were used: 2 D EPI BOLD: TE:
644 29.0 ms, TR: 1679.00 ms, FOV: 22.4 * 22.4 cm, flip angle: 70°, s1: 2 mm, TA: 20:17

min, fat saturation, 715 volumes in total; 2 D field map sequence: TR: 594 ms, TE1: 5.51 ms, TE2: 7.79 ms, FOV: 22.4 * 22.4 cm, flip angle: 40°, s1: 2 mm, TA: 1:31 min.

EEG Data

Continuous EEG data was recorded inside the MRI scanner using a custom 64-channel BrainCap-MR for 3 Tesla using BrainVision Recorder (Version 1.10, BrainProducts, Gilching, Germany). The cap contained 64 passive sintered Ag/AgCl electrodes arranged according to the 10/20 System, as well as one ECG electrode. FCz served as the reference and Pz served as the ground electrode. The cap was connected to two Brain Amp MR plus amplifier systems with 32 channels each (BrainProducts, Gilching, Germany), powered by one rechargeable battery unit. Amplifiers and the battery unit were positioned on foam cushions directly behind the head coil inside the scanner. Electrode skin impedance was kept below 10 kΩ. EEG data was recorded with a sampling rate of 5,000 Hz and an amplitude resolution of 0.5 µV for EEG channels and 10 µV for the ECG channel. The EEG system was synchronized with the clock of the MRI system using a SyncBox (BrainProducts, Gilching, Germany). The helium pump of the MRI system was switched off during data recording. Data was transmitted from the amplifiers to the recording computer outside of the scanner room via a fiber-optic cable.

4.3. Preprocessing

Electrodermal Data

Preprocessing and analysis of electrodermal data were performed using the Ledalab toolbox for MATLAB (Benedek & Kaernbach, 2010). Single-subject data was downsampled to 100 Hz and visually screened. In total, 21 subjects were excluded

670 from the electrodermal analysis (18 due to physiological non-responsiveness, 3 due to
671 equipment malfunction). From the remaining 26 subjects, all data segments around
672 pain stimulation were screened for excessive artifacts, resulting in the exclusion of 55
673 of the 2340 segments (2.35%). Using a deconvolution method implemented in
674 Ledalab, raw electrodermal data were decomposed into continuous phasic (driver) and
675 tonic components. Subsequent analyses were performed on the extracted phasic skin
676 conductance responses (SCRs). The response window for pain was determined by
677 visual inspection of the curve to cover the peak and set between 2 and 7.5 s. SCR
678 segments within the response window were log- and z-transformed within participants.
679 For the log-transform, a constant (minimum of the driver plus 1) was added to the data
680 to shift it to positive values. Lastly, segments were averaged per subject for each of
681 the three conditions.

682

683 **fMRI Data**

684 Preprocessing of fMRI data was done using the Statistical Parameter Mapping
685 software (SPM 12, Wellcome Department of Imaging Neuroscience, London, UK,
686 https://www.fil.ion.ucl.ac.uk/spm/software/spm12/). The first two volumes of each
687 block were dropped to get full MRI saturation effects. Further, realignment and
688 unwarping, registration to standard space (Montreal Neurological Institute), and spatial
689 smoothing with a 6 mm Gaussian kernel were used on the data.

690

691 **EEG Data**

692 MR and cardioballistic artifacts were corrected using BrainVision Analyzer 2.2
693 (BrainProducts, Gilching, Germany) for each block separately. Continuous MR artifacts
694 were corrected with sliding baseline corrected average templates. Data was then

downsampled to 500 Hz. Cardioballistic artifact correction was done by semi-automatically detecting a pulse template, marking it in the electrocardiogram channel, and then subtracting it from recordings.

For the remaining preprocessing and analysis, we used the Fieldtrip toolbox for Matlab (Oostenveld et al., 2011). Data were cut into trials including all relevant time intervals from 1,000 ms before cue onset to the end of pain 15,800 ms after cue onset. The resulting segmented data were low-pass filtered at 150 Hz and high-pass filtered at 0.5 Hz. We adapted a recent preprocessing approach introduced by Hipp et al. (2011). The data was split into low- and high-frequency data (34 Hz low-pass filter and 16 Hz high-pass filter, respectively) and processed in parallel. This approach leads to high sensitivity in detecting and removing artifacts from the data as e.g. heartbeats cause more artifacts at lower frequencies and muscle activity affects higher frequencies more strongly. All trials were visually inspected and removed for both subsets when containing large artifacts. Then, both high- and low-frequency data were subjected to an independent component analysis (ICA) using a logistic infomax algorithm. Components reflecting residual cardioballistic and MR artifacts, blinks, eye- and head movement, and muscle activity were identified by visual inspection of the time course, spectrum, and topography of each component and discarded. Both subsets were re-referenced to the average of all channels and the original reference electrode was regained. Lastly, we subjected all data to another full visual scan and shifted the time axis so that the onset of pain stimulation occurred at $t = 0$ s. In total, the visual artifact screening led to the exclusion of 228 of the 3944 recorded trials (5.78%).

719 ***Time-frequency decomposition***

720 Our procedure was again adapted from Hipp et al. (2011). Time-frequency
721 decomposition was conducted for 21 logarithmically spaced frequencies ranging from
722 4 to 128 Hz (0.25-octave increments) in 0.1 s steps using the multi-taper method based
723 on discrete prolate spheroid sequences (DPSS). The high-frequency data were used
724 for the frequency transformation of frequencies above 25 Hz, and the low-frequency
725 data for frequencies below 25 Hz. Temporal and spectral smoothing were adjusted to
726 match 250 ms and 3/4 octave, respectively. This was achieved by fixing the time
727 window to 250 ms and adjusting the number of Slepian tapers for frequencies larger
728 than 16 Hz, while for frequencies up to 16 Hz, a single taper was used, and the time
729 window was adjusted. We extracted single-trial time-frequency resolved data for each
730 participant.

731

732 **4.4. Data analysis**

733 **Behavioral Data**

734 We compared differences in pain and expectation ratings for the different cue
735 conditions by computing two repeated-measures ANOVAs with cue type (placebo vs.
736 nocebo vs. control) as predictor and pain and expectation ratings as outcome,
737 respectively. Partial eta-squared is used to describe effect sizes.

738 Furthermore, we analyzed variability within conditions indicated by the relative
739 variability index (Mestdagh et al., 2018) by computing two repeated-measures ANOVA
740 with cue type (placebo vs. nocebo vs. control) and measurement block (block 1, block
741 2, block 3) for the relative variability index of expectation and pain ratings, respectively.

742

743 **Electrodermal Data**

744 We compared differences in SCRs in the pain phase by conducting a repeated-
745 measures ANOVA with the factor cue type (placebo vs. nocebo vs. control) as predictor
746 and SCR as outcome.

747

748 **fMRI Data**

749 ***Statistical inference***

750 For each subject, a Finite Impulse Response model (FIR model) was set up on
751 a time course of 18.4 s starting at the onset of the cue, divided into 11 bins, with a bin
752 roughly covering the duration of one TR (1.679 s compared to 1.675 s). The FIR model
753 was implemented separately for each condition. Data was also corrected for
754 cardioballistic and respiratory artifacts by including them as regressors built with the
755 RETROICOR algorithm of the PhysIO toolbox (Frässle et al., 2021; Kasper et al.,
756 2017).

757 On the group level in a flexible factorial design, directed *t*-contrasts were set up
758 for common effects (placebo and nocebo vs. control), exclusively masked with the *F*-
759 contrast between placebo and nocebo (thresholded at $p < .05$ uncorrected) to identify
760 areas that showed a similar response for placebo and nocebo but different to the
761 control condition in the anticipation phase. For the comparison between placebo and
762 nocebo, directed *t*-contrasts were set up to identify areas that showed distinct
763 modulation by placebo and nocebo in both anticipation and pain phase. Analyses in
764 the anticipation phase were performed by including the FIR regressors covering the
765 time period from -4.275 s until -0.925 s relative to pain onset (bins 4 and 5), analyses
766 in the pain phase by including the FIR regressors covering the time from 0.75 s until

767 5.8 s relative to pain onset (bins 7, 8 and 9). All analyses were corrected for multiple
768 comparisons using FWE ($p < 0.05$) correction.

769

770 ***ROI analyses***

771 Additionally, ROI analyses were conducted regarding a priori hypotheses in the
772 following areas defined by the anatomy based on the Harvard-Oxford atlas: insular
773 cortex, thalamus, ACC, hippocampus and amygdala. Furthermore, a ROI analysis was
774 conducted on the DLPFC based on the clusters identified in the meta-analysis
775 conducted by Zunhammer et al. (2021) by applying a 15 mm-radius sphere around the
776 two reported peak coordinates (xyz_{MNI}: 42, 11, 33 and xyz_{MNI}: -30, 13, 54) bilaterally.

777

778 **Combined EEG-fMRI Analysis**

779 Single-trial fMRI BOLD response amplitudes were estimated based on the pre-
780 processed MR data using GLMsingle (Prince et al., 2022). The hemodynamic
781 response during the anticipation phase was estimated by fitting a boxcar function with
782 a length of 1.679 s to the anticipation onset. The accuracy of beta estimates was
783 improved by an adaptation of GLMdenoise for single-trial beta estimation. Further,
784 noise was reduced by using fractional ridge regression as integrated in the GLMsingle
785 toolbox. For each trial, we extracted the mean beta within several regions of interest
786 centered around the significant peak voxels derived from the MR analyses of common
787 effects of expectations during the anticipation phase. These included the left anterior
788 insula (xyz_{MNI}: -28, 22, -6), left (xyz_{MNI}: -2, 40, -4) and right ACC (xyz_{MNI}: 4, 42, 12),
789 right vmPFC (xyz_{MNI}: 14, 56, -14), left (xyz_{MNI}: -32, 18, 36) and right DLPFC (xyz_{MNI}:
790 40, 24, 36), and left thalamus (-6, -12, 4; all with 10mm sphere). For each participant

on a single-trial level, Spearman's rank correlation coefficients between beta ROI estimates and time-frequency EEG data were computed, resulting in one time-frequency-resolved correlation pattern per participant and ROI. For the group level analysis, correlations were Fisher-z-transformed and tested against zero using nonparametric cluster-based permutation tests as implemented in the Fieldtrip toolbox (cluster threshold: $p = 0.05$, minimum neighbors: 2, number of randomizations: 2000). Statistics were calculated from cue onset until pain offset (-9.3 until 3.9 s relative to pain onset).

5. Data Availability

Derived data that support the findings of this study are available at https://osf.io/3g49v/. For additional information and requests, please contact the lead researcher directly.

6. Acknowledgements

This research is funded by the Deutsche Forschungsgemeinschaft (DFG, German Research Foundation): TRR 289 Treatment Expectation — Project Number 422744262, Project A03.

7. Author contributions

C.A.W.: Software, Validation, Formal Analysis, Investigation, Data Curation, Writing - Original Draft, Writing — Review and Editing, Visualization; M.W.: Software, Validation, Formal Analysis, Investigation, Data Curation, Writing — Original Draft,

Writing — Review and Editing, Visualization; M.R.: Conceptualization, Methodology, Software, Validation, Resources, Writing — Review and Editing, Supervision, Project administration, Funding acquisition.

C.A.W. and M.W. contributed equally to this work.

8. References

Adler-Neal, A. L., Emerson, N. M., Farris, S. R., Jung, Y., Coghill, R. C., & Zeidan, F. (2019). Brain moderators supporting the relationship between depressive mood and pain. *Pain*, *160*(9), 2028–2035. https://doi.org/10.1097/j.pain.0000000000001595

Amanzio, M., Benedetti, F., Porro, C. A., Palermo, S., & Cauda, F. (2013). Activation likelihood estimation meta-analysis of brain correlates of placebo analgesia in human experimental pain. *Human Brain Mapping*, *34*(3), 738–752. https://doi.org/10.1002/hbm.21471

Amanzio, M., & Palermo, S. (2019). Pain Anticipation and Nocebo-Related Responses: A Descriptive Mini-Review of Functional Neuroimaging Studies in Normal Subjects and Precious Hints on Pain Processing in the Context of Neurodegenerative Disorders. *Frontiers in Pharmacology*, *10*, 969. https://doi.org/10.3389/fphar.2019.00969

Atlas, L. Y., & Wager, T. D. (2012). How expectations shape pain. *Neuroscience Letters*, *520*(2), 140–148. https://doi.org/10.1016/j.neulet.2012.03.039

Atlas, L. Y., & Wager, T. D. (2014). A meta-analysis of brain mechanisms of placebo analgesia: Consistent findings and unanswered questions. *Handbook of Experimental Pharmacology*, *225*, 37–69. https://doi.org/10.1007/978-3-662-44519-8_3

Beck, A. T., Steer, R. A., & Brown, G. K. (1996). *Manual for the Beck Depression Inventory-II*. Psychological Corporation.

Benedek, M., & Kaernbach, C. (2010). A continuous measure of phasic electrodermal activity. *Journal of Neuroscience Methods*, *190*(1), 80–91. https://doi.org/10.1016/j.jneumeth.2010.04.028

Benedetti, F. (2014). Placebo effects: From the neurobiological paradigm to translational implications. *Neuron*, *84*(3), 623–637. https://doi.org/10.1016/j.neuron.2014.10.023

Benedetti, F., Frisaldi, E., Barbiani, D., Camerone, E., & Shaibani, A. (2020). Nocebo and the contribution of psychosocial factors to the generation of pain. *Journal of Neural Transmission (Vienna, Austria : 1996)*, *127*(4), 687–696. https://doi.org/10.1007/s00702-019-02104-x

Bingel, U., Wanigasekera, V., Wiech, K., Ni Mhuircheartaigh, R., Lee, M. C., Ploner, M., & Tracey, I. (2011). The effect of treatment expectation on drug efficacy: Imaging the analgesic benefit of the opioid remifentanil. *Science Translational Medicine*, *3*(70), 70ra14. https://doi.org/10.1126/scitranslmed.3001244

Botvinik-Nezer, R., Petre, B., Ceko, M., Lindquist, M. A., Friedman, N. P., & Wager, T. D. (2023). Placebo treatment affects brain systems related to affective and cognitive processes, but not nociceptive pain. *BioRxiv*, 2023.09.21.558825. https://doi.org/10.1101/2023.09.21.558825

Büchel, C., Geuter, S., Sprenger, C., & Eippert, F. (2014). Placebo analgesia: A predictive coding perspective. *Neuron*, *81*(6), 1223–1239. https://doi.org/10.1016/j.neuron.2014.02.042

Colloca, L., & Benedetti, F. (2007). Nocebo hyperalgesia: How anxiety is turned into pain. *Current Opinion in Anaesthesiology*, *20*(5), 435–439. https://doi.org/10.1097/ACO.0b013e3282b972fb

Colloca, L., Petrovic, P., Wager, T. D., Ingvar, M., & Benedetti, F. (2010). How the number of learning trials affects placebo and nocebo responses. *Pain*, *151*(2), 430–439. https://doi.org/10.1016/j.pain.2010.08.007

Colloca, L., Sigaudo, M., & Benedetti, F. (2008). The role of learning in nocebo and placebo effects. *Pain*, *136*(1-2), 211–218. https://doi.org/10.1016/j.pain.2008.02.006

Craggs, J. G., Price, D. D., & Robinson, M. E. (2014). Enhancing the placebo response: Functional magnetic resonance imaging evidence of memory and semantic processing in placebo analgesia. *The Journal of Pain*, *15*(4), 435–446. https://doi.org/10.1016/j.jpain.2013.12.009

Crawford, L. S., Mills, E. P., Hanson, T., Macey, P. M., Glarin, R., Macefield, V. G., Keay, K. A., & Henderson, L. A. (2021). Brainstem Mechanisms of Pain Modulation: A within-Subjects 7T fMRI Study of Placebo Analgesic and Nocebo Hyperalgesic Responses. *Journal of Neuroscience*, *41*(47), 9794–9806. https://doi.org/10.1523/JNEUROSCI.0806-21.2021

Dionisio, S., Mayoglou, L., Cho, S.-M., Prime, D., Flanigan, P. M., Lega, B., Mosher, J., Leahy, R., Gonzalez-Martinez, J., & Nair, D. (2019). Connectivity of the human insula: A cortico-cortical evoked potential (CCEP) study. *Cortex; a Journal Devoted to the Study of the Nervous System and Behavior*, *120*, 419–442. https://doi.org/10.1016/j.cortex.2019.05.019

Egorova, N., Yu, R., Kaur, N., Vangel, M., Gollub, R. L., Dougherty, D. D., Kong, J., & Camprodon, J. A. (2015). Neuromodulation of conditioned placebo/nocebo in heat pain: Anodal vs cathodal transcranial direct current stimulation to the right dorsolateral prefrontal cortex. *Pain*, *156*(7), 1342–1347. https://doi.org/10.1097/j.pain.0000000000000163

Eippert, F., Bingel, U., Schoell, E. D., Yacubian, J., Klinger, R., Lorenz, J., & Büchel, C. (2009). Activation of the opioidergic descending pain control system underlies placebo analgesia. *Neuron*, *63*(4), 533–543. https://doi.org/10.1016/j.neuron.2009.07.014

Englert, R., Schedlowski, M., Engler, H., Rief, W., Büchel, C., Bingel, U., & Spisak, T. (2023). ALIIAS: Anonymization/Pseudonymization with LimeSurvey integration and II-factor Authentication for Scientific research. *SoftwareX*, *24*, 101522. https://doi.org/10.1016/j.softx.2023.101522

Frässle, S., Aponte, E. A., Bollmann, S [Saskia], Brodersen, K. H., Do, C. T., Harrison, O. K., Harrison, S. J., Heinzle, J., Iglesias, S., Kasper, L., Lomakina, E. I., Mathys, C., Müller-Schrader, M., Pereira, I., Petzschner, F. H., Raman, S., Schöbi, D., Toussaint, B., Weber, L. A., . . . Stephan, K. E. (2021). Tapas: An Open-Source Software Package for Translational Neuromodeling and Computational Psychiatry. *Frontiers in Psychiatry*, *12*, 680811. https://doi.org/10.3389/fpsyt.2021.680811

Freeman, S., Yu, R., Egorova, N., Chen, X., Kirsch, I., Claggett, B., Kaptchuk, T. J., Gollub, R. L., & Kong, J. (2015). Distinct neural representations of placebo and nocebo effects. *NeuroImage*, *112*, 197–207. https://doi.org/10.1016/j.neuroimage.2015.03.015

Frisaldi, E., Piedimonte, A., & Benedetti, F. (2015). Placebo and nocebo effects: A complex interplay between psychological factors and neurochemical networks. *The American Journal of Clinical Hypnosis*, *57*(3), 267–284. https://doi.org/10.1080/00029157.2014.976785

Fu, J., Wu, S., Liu, C., Camilleri, J. A., Eickhoff, S. B., & Yu, R. (2021). Distinct neural networks subserve placebo analgesia and nocebo hyperalgesia. *NeuroImage*, *231*, 117833. https://doi.org/10.1016/j.neuroimage.2021.117833

Fullana, M. A., Harrison, B. J., Soriano-Mas, C., Vervliet, B., Cardoner, N., Àvila-Parcet, A., & Radua, J. (2016). Neural signatures of human fear conditioning: An updated and extended meta-analysis of fMRI studies. *Molecular Psychiatry*, *21*(4), 500–508. https://doi.org/10.1038/mp.2015.88

Geuter, S., Eippert, F., Hindi Attar, C., & Büchel, C. (2013). Cortical and subcortical responses to high and low effective placebo treatments. *NeuroImage*, *67*, 227–236. https://doi.org/10.1016/j.neuroimage.2012.11.029

Geuter, S., Koban, L., & Wager, T. D. (2017). The Cognitive Neuroscience of Placebo Effects: Concepts, Predictions, and Physiology. *Annual Review of Neuroscience*, *40*, 167–188. https://doi.org/10.1146/annurev-neuro-072116-031132

Hautzinger, M., Keller, F., & Kühner, C. (2006). *Beck Depressions-Inventar (BDI-II). Revision.* Harcourt Test Services.

Hipp, J. F., Engel, A. K., & Siegel, M. (2011). Oscillatory synchronization in large-scale cortical networks predicts perception. *Neuron*, *69*(2), 387–396. https://doi.org/10.1016/j.neuron.2010.12.027

Horing, B., & Büchel, C. (2022). The human insula processes both modality-independent and pain-selective learning signals. *PLoS Biology*, *20*(5), e3001540. https://doi.org/10.1371/journal.pbio.3001540

Jablonowski, J., & Rose, M. (2022). The functional dissociation of posterior parietal regions during multimodal memory formation. *Human Brain Mapping*, *43*(11), 3469–3485. https://doi.org/10.1002/hbm.25861

Kasper, L., Bollmann, S [Steffen], Diaconescu, A. O., Hutton, C., Heinzle, J., Iglesias, S., Hauser, T. U., Sebold, M., Manjaly, Z.-M., Pruessmann, K. P., & Stephan, K. E. (2017). The PhysIO Toolbox for Modeling Physiological Noise in fMRI Data. *Journal of Neuroscience Methods*, *276*, 56–72. https://doi.org/10.1016/j.jneumeth.2016.10.019

Kilner, J. M., Mattout, J., Henson, R., & Friston, K. J. (2005). Hemodynamic correlates of EEG: A heuristic. *NeuroImage*, *28*(1), 280–286. https://doi.org/10.1016/j.neuroimage.2005.06.008

Koban, L., Jepma, M., Geuter, S., & Wager, T. D. (2017). What's in a word? How instructions, suggestions, and social information change pain and emotion. *Neuroscience and Biobehavioral Reviews*, *81*(Pt A), 29–42. https://doi.org/10.1016/j.neubiorev.2017.02.014

Kober, H., Barrett, L. F., Joseph, J., Bliss-Moreau, E., Lindquist, K., & Wager, T. D. (2008). Functional grouping and cortical-subcortical interactions in emotion: A meta-analysis of neuroimaging studies. *NeuroImage*, *42*(2), 998–1031. https://doi.org/10.1016/j.neuroimage.2008.03.059

Kong, J., & Benedetti, F. (2014). Placebo and nocebo effects: An introduction to psychological and biological mechanisms. *Handbook of Experimental Pharmacology*, *225*, 3–15. https://doi.org/10.1007/978-3-662-44519-8_1

Kong, J., Gollub, R. L., Polich, G., Kirsch, I., Laviolette, P., Vangel, M., Rosen, B., & Kaptchuk, T. J. (2008). A functional magnetic resonance imaging study on the neural mechanisms of hyperalgesic nocebo effect. *Journal of Neuroscience*, *28*(49), 13354–13362. https://doi.org/10.1523/JNEUROSCI.2944-08.2008

Kong, J., Kaptchuk, T. J., Polich, G., Kirsch, I., & Gollub, R. L. (2007). Placebo analgesia: Findings from brain imaging studies and emerging hypotheses. *Reviews in the Neurosciences*, *18*(3-4), 173–190. https://doi.org/10.1515/REVNEURO.2007.18.3-4.173

Koyama, T., McHaffie, J. G., Laurienti, P. J., & Coghill, R. C. (2005). The subjective experience of pain: Where expectations become reality. *Proceedings of the National Academy of Sciences of the United States of America*, *102*(36), 12950–12955. https://doi.org/10.1073/pnas.0408576102

Krummenacher, P., Candia, V., Folkers, G., Schedlowski, M., & Schönbächler, G. (2010). Prefrontal cortex modulates placebo analgesia. *Pain*, *148*(3), 368–374. https://doi.org/10.1016/j.pain.2009.09.033

Laux, L., Hock, M., Bergner-Koether, R., Hodapp, V., & Renner, K.-H. (2013). *Das State-Trait-Angst-Depressions-Inventar: STADI; Manual.* Hogrefe.

Lee, J.-J., Lee, S., Lee, D. H., & Woo, C.-W. (2022). Functional brain reconfiguration during sustained pain. *ELife*, *11.* https://doi.org/10.7554/eLife.74463

Livrizzi, G., Lubejko, S. T., Johnson, D. A., Weiss, C. E., Patel, J., & Banghart, M. R. (2022). Prefrontal Input to the Periaqueductal Gray Controls Placebo Analgesia. *The Journal of Pain*, *23*(5), 19–20. https://doi.org/10.1016/j.jpain.2022.03.076

Lu, C., Yang, T., Zhao, H., Zhang, M., Meng, F., Fu, H., Xie, Y., & Xu, H. (2016). Insular Cortex is Critical for the Perception, Modulation, and Chronification of Pain. *Neuroscience Bulletin*, *32*(2), 191–201. https://doi.org/10.1007/s12264-016-0016-y

Manaï, M., van Middendorp, H., Veldhuijzen, D. S., Huizinga, T. W. J., & Evers, A. W. M. (2019). How to prevent, minimize, or extinguish nocebo effects in pain: A narrative review on mechanisms, predictors, and interventions. *Pain Reports*, *4*(3), e699. https://doi.org/10.1097/PR9.0000000000000699

McNeil, D. W., & Rainwater, A. J. (1998). Development of the Fear of Pain Questionnaire--III. *Journal of Behavioral Medicine*, *21*(4), 389–410. https://doi.org/10.1023/A:1018782831217

Mestdagh, M., Pe, M., Pestman, W., Verdonck, S., Kuppens, P., & Tuerlinckx, F. (2018). Sidelining the mean: The relative variability index as a generic mean-corrected variability measure for bounded variables. *Psychological Methods*, *23*(4), 690–707. https://doi.org/10.1037/met0000153

Nickel, M. M., Tiemann, L., Hohn, V. D., May, E. S., Gil Ávila, C., Eippert, F., & Ploner, M. (2022). Temporal-spectral signaling of sensory information and expectations in the cerebral processing of pain. *Proceedings of the National Academy of Sciences of the United States of America*, *119*(1). https://doi.org/10.1073/pnas.2116616119

Oostenveld, R., Fries, P., Maris, E., & Schoffelen, J.-M. (2011). Fieldtrip: Open source software for advanced analysis of MEG, EEG, and invasive

electrophysiological data. *Computational Intelligence and Neuroscience*, *2011*, 156869. https://doi.org/10.1155/2011/156869

Palermo, S., Benedetti, F., Costa, T., & Amanzio, M. (2015). Pain anticipation: An activation likelihood estimation meta-analysis of brain imaging studies. *Human Brain Mapping*, *36*(5), 1648–1661. https://doi.org/10.1002/hbm.22727

Ploghaus, A., Tracey, I., Gati, J. S., Clare, S., Menon, R. S., Matthews, P. M., & Rawlins, J. N. (1999). Dissociating pain from its anticipation in the human brain. *Science (New York, N.Y.)*, *284*(5422), 1979–1981. https://doi.org/10.1126/science.284.5422.1979

Ploner, M., Sorg, C., & Gross, J. (2017). Brain Rhythms of Pain. *Trends in Cognitive Sciences*, *21*(2), 100–110. https://doi.org/10.1016/j.tics.2016.12.001

Prince, J. S., Charest, I., Kurzawski, J. W., Pyles, J. A., Tarr, M. J., & Kay, K. N. (2022). Improving the accuracy of single-trial fMRI response estimates using GLMsingle. *ELife*, *11.* https://doi.org/10.7554/eLife.77599

Rossettini, G., Campaci, F., Bialosky, J., Huysmans, E., Vase, L., & Carlino, E. (2023). The Biology of Placebo and Nocebo Effects on Experimental and Chronic Pain: State of the Art. *Journal of Clinical Medicine*, *12*(12). https://doi.org/10.3390/jcm12124113

Schmid, J., Bingel, U., Ritter, C., Benson, S., Schedlowski, M., Gramsch, C., Forsting, M., & Elsenbruch, S. (2015). Neural underpinnings of nocebo hyperalgesia in visceral pain: A fMRI study in healthy volunteers. *NeuroImage*, *120*, 114–122. https://doi.org/10.1016/j.neuroimage.2015.06.060

Scott, D. J., Stohler, C. S., Egnatuk, C. M., Wang, H., Koeppe, R. A., & Zubieta, J.-K. (2008). Placebo and nocebo effects are defined by opposite opioid and dopaminergic responses. *Archives of General Psychiatry*, *65*(2), 220–231. https://doi.org/10.1001/archgenpsychiatry.2007.34

Shi, Y., Cui, S., Zeng, Y., Huang, S., Cai, G., Yang, J., & Wu, W. (2021). Brain Network to Placebo and Nocebo Responses in Acute Experimental Lower Back Pain: A Multivariate Granger Causality Analysis of fMRI Data. *Frontiers in Behavioral Neuroscience*, *15*, 696577. https://doi.org/10.3389/fnbeh.2021.696577

Shih, Y.-W., Tsai, H.-Y., Lin, F.-S., Lin, Y.-H., Chiang, C.-Y., Lu, Z.-L., & Tseng, M.-T. (2019). Effects of Positive and Negative Expectations on Human Pain Perception Engage Separate But Interrelated and Dependently Regulated Cerebral Mechanisms. *Journal of Neuroscience*, *39*(7), 1261–1274. https://doi.org/10.1523/JNEUROSCI.2154-18.2018

Skvortsova, A., Veldhuijzen, D. S., van Middendorp, H., Colloca, L., & Evers, A. W. M. (2020). Effects of Oxytocin on Placebo and Nocebo Effects in a Pain Conditioning Paradigm: A Randomized Controlled Trial. *The Journal of Pain*, *21*(3-4), 430–439. https://doi.org/10.1016/j.jpain.2019.08.010

Strube, A., Rose, M., Fazeli, S., & Büchel, C. (2021). The temporal and spectral characteristics of expectations and prediction errors in pain and thermoception. *ELife*, *10.* https://doi.org/10.7554/eLife.62809

Taesler, P., & Rose, M. (2016). Prestimulus Theta Oscillations and Connectivity Modulate Pain Perception. *Journal of Neuroscience*, *36*(18), 5026–5033. https://doi.org/10.1523/JNEUROSCI.3325-15.2016

Tu, Y., Park, J., Ahlfors, S. P., Khan, S., Egorova, N., Lang, C., Cao, J., & Kong, J. (2019). A neural mechanism of direct and observational conditioning for

placebo and nocebo responses. *NeuroImage*, *184*, 954–963. https://doi.org/10.1016/j.neuroimage.2018.10.020

Tu, Y., Wilson, G., Camprodon, J., Dougherty, D. D., Vangel, M., Benedetti, F., Kaptchuk, T. J., Gollub, R. L., & Kong, J. (2021). Manipulating placebo analgesia and nocebo hyperalgesia by changing brain excitability. *Proceedings of the National Academy of Sciences of the United States of America*, *118*(19), e2101273118. https://doi.org/10.1073/pnas.2101273118

Tu, Y., Zhang, L., & Kong, J. (2022). Placebo and nocebo effects: From observation to harnessing and clinical application. *Translational Psychiatry*, *12*(1), 524. https://doi.org/10.1038/s41398-022-02293-2

Tu, Y., Zhang, Z., Tan, A., Peng, W., Hung, Y. S., Moayedi, M., Iannetti, G. D., & Hu, L. (2016). Alpha and gamma oscillation amplitudes synergistically predict the perception of forthcoming nociceptive stimuli. *Human Brain Mapping*, *37*(2), 501–514. https://doi.org/10.1002/hbm.23048

Vilberg, K. L., & Rugg, M. D. (2012). The neural correlates of recollection: Transient versus sustained FMRI effects. *Journal of Neuroscience*, *32*(45), 15679–15687. https://doi.org/10.1523/JNEUROSCI.3065-12.2012

Wager, T. D., & Atlas, L. Y. (2015). The neuroscience of placebo effects: Connecting context, learning and health. *Nature Reviews Neuroscience*, *16*(7), 403–418. https://doi.org/10.1038/nrn3976

Wager, T. D., Atlas, L. Y., Leotti, L. A., & Rilling, J. K. (2011). Predicting individual differences in placebo analgesia: Contributions of brain activity during anticipation and pain experience. *Journal of Neuroscience*, *31*(2), 439–452. https://doi.org/10.1523/JNEUROSCI.3420-10.2011

Wager, T. D., Rilling, J. K., Smith, E. E., Sokolik, A., Casey, K. L., Davidson, R. J., Kosslyn, S. M., Rose, R. M., & Cohen, J. D. (2004). Placebo-induced changes in FMRI in the anticipation and experience of pain. *Science (New York, N.Y.)*, *303*(5661), 1162–1167. https://doi.org/10.1126/science.1093065

Watson, A., El-Deredy, W., Iannetti, G. D., Lloyd, D., Tracey, I., Vogt, B. A., Nadeau, V., & Jones, A. K. P. (2009). Placebo conditioning and placebo analgesia modulate a common brain network during pain anticipation and perception. *Pain*, *145*(1-2), 24–30. https://doi.org/10.1016/j.pain.2009.04.003

Wiech, K., Lin, C., Brodersen, K. H., Bingel, U., Ploner, M., & Tracey, I. (2010). Anterior insula integrates information about salience into perceptual decisions about pain. *Journal of Neuroscience*, *30*(48), 16324–16331. https://doi.org/10.1523/JNEUROSCI.2087-10.2010

Woo, C.-W., Schmidt, L., Krishnan, A., Jepma, M., Roy, M., Lindquist, M. A., Atlas, L. Y., & Wager, T. D. (2017). Quantifying cerebral contributions to pain beyond nociception. *Nature Communications*, *8*(1), 14211. https://doi.org/10.1038/ncomms14211

Zunhammer, M., Spisák, T., Wager, T. D., & Bingel, U. (2021). Meta-analysis of neural systems underlying placebo analgesia from individual participant fMRI data. *Nature Communications*, *12*(1), 1391. https://doi.org/10.1038/s41467-021-21179-3

9. Figures

Figure 1

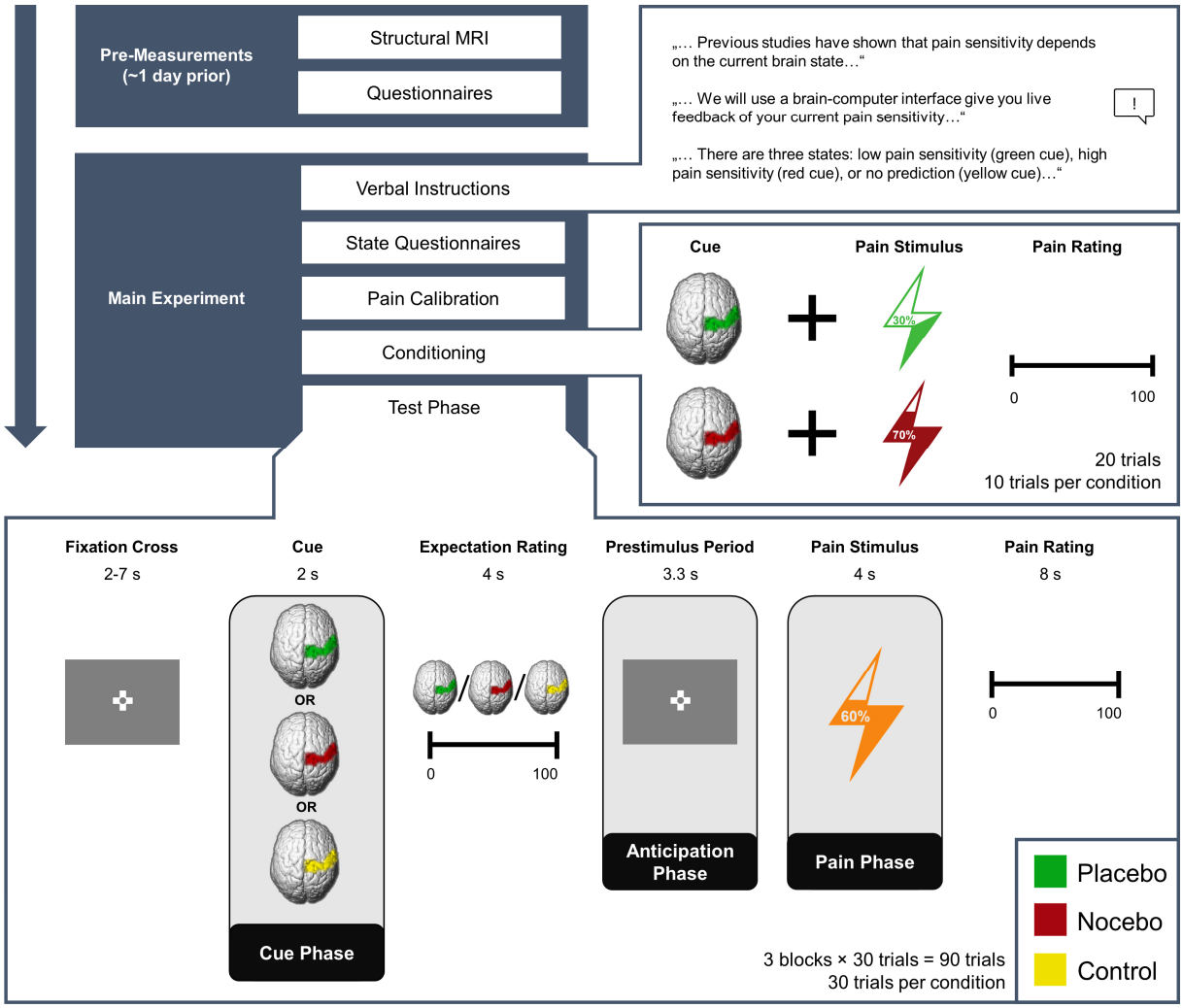

Experimental Procedure.

Structure of the experiment including pre-measurements and the main experiment. Expectations were generated using a sham BCI, i.e., participants were told that they would receive real-time feedback regarding their pain sensitivity (verbal instructions) and experienced the validity of this feedback (conditioning). In the conditioning phase, green cues were paired with lower pain intensities compared to red cues unbeknownst to the participants. In the test phase, the stimulation temperature was always the same, regardless of the cue. The presentation of the condition cue varied from trial to trial.

Figure 2

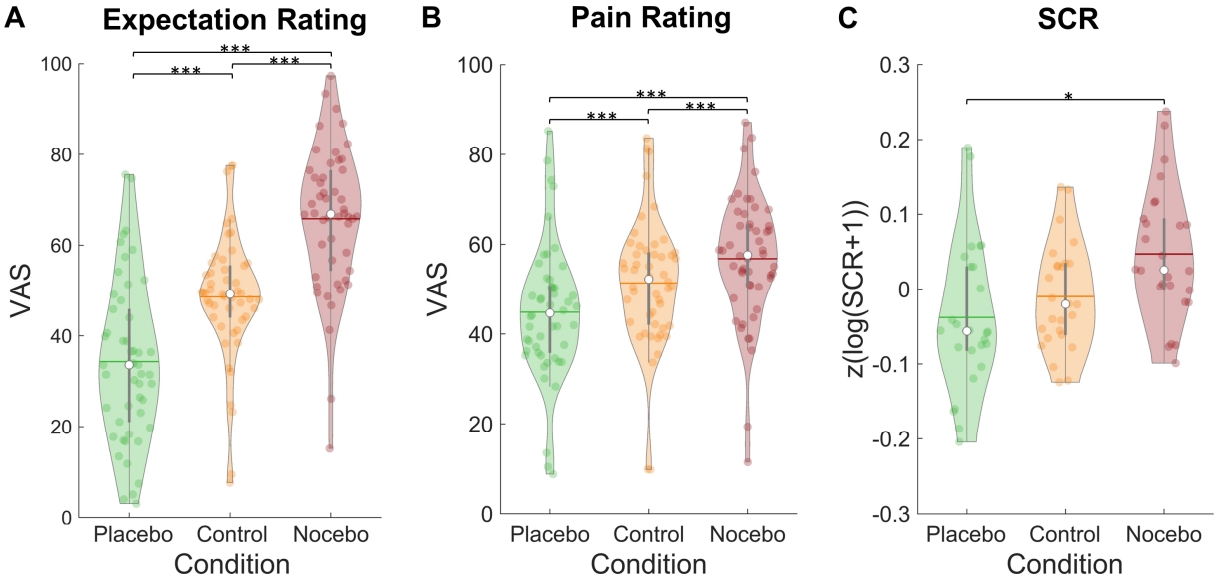

Expectation ratings, pain ratings and skin conductance response by condition. Mean expectation **(A)** and pain ratings **(B)** on a visual analogue scale separately for each condition. **(C)** Mean skin conductance responses in the three conditions. White dots = mean, horizontal lines = median, thick grey vertical lines = upper and lower quartile, coloured dots = pain ratings of individual participants per condition.

* $p < .05$. ** $p < .01$. *** $p < .001$.

Figure 3

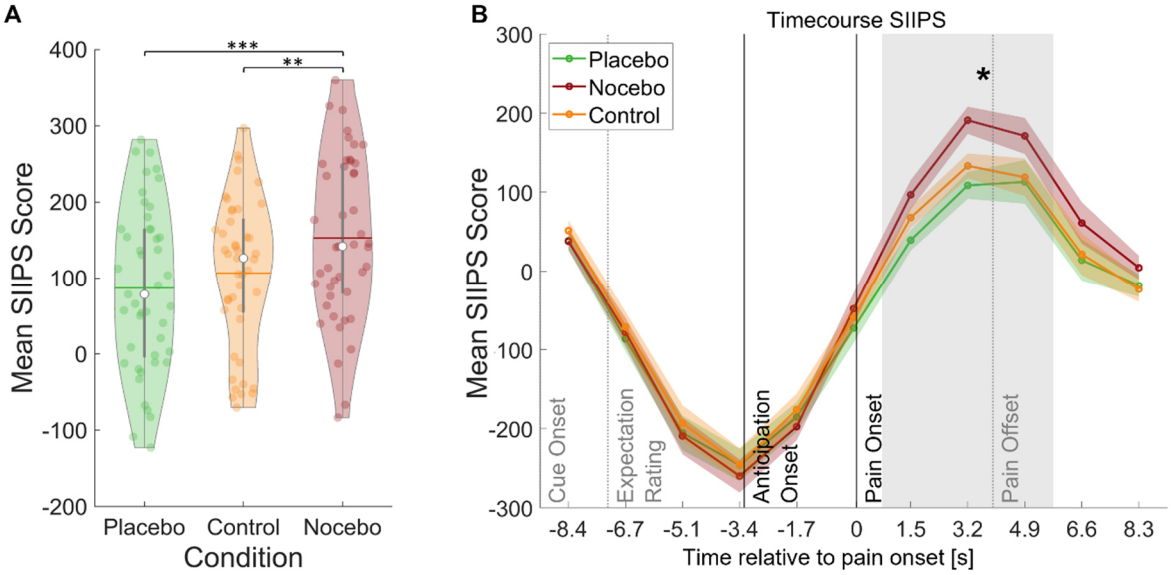

SIIPS scores by condition.

(A) Mean SIIPS score per condition for all time-points during pain perception. White dots = mean, horizontal lines = median, thick grey vertical lines = upper and lower quartile, coloured dots = pain ratings of individual participants per condition. * $p < .05$. ** $p < .01$. *** $p < .001$. **(B)** Mean SIIPS score per condition plotted over the duration of the whole trial. The mean SIIPS scores shown in A were extracted from the grey marked period.

1150 **Figure 4**

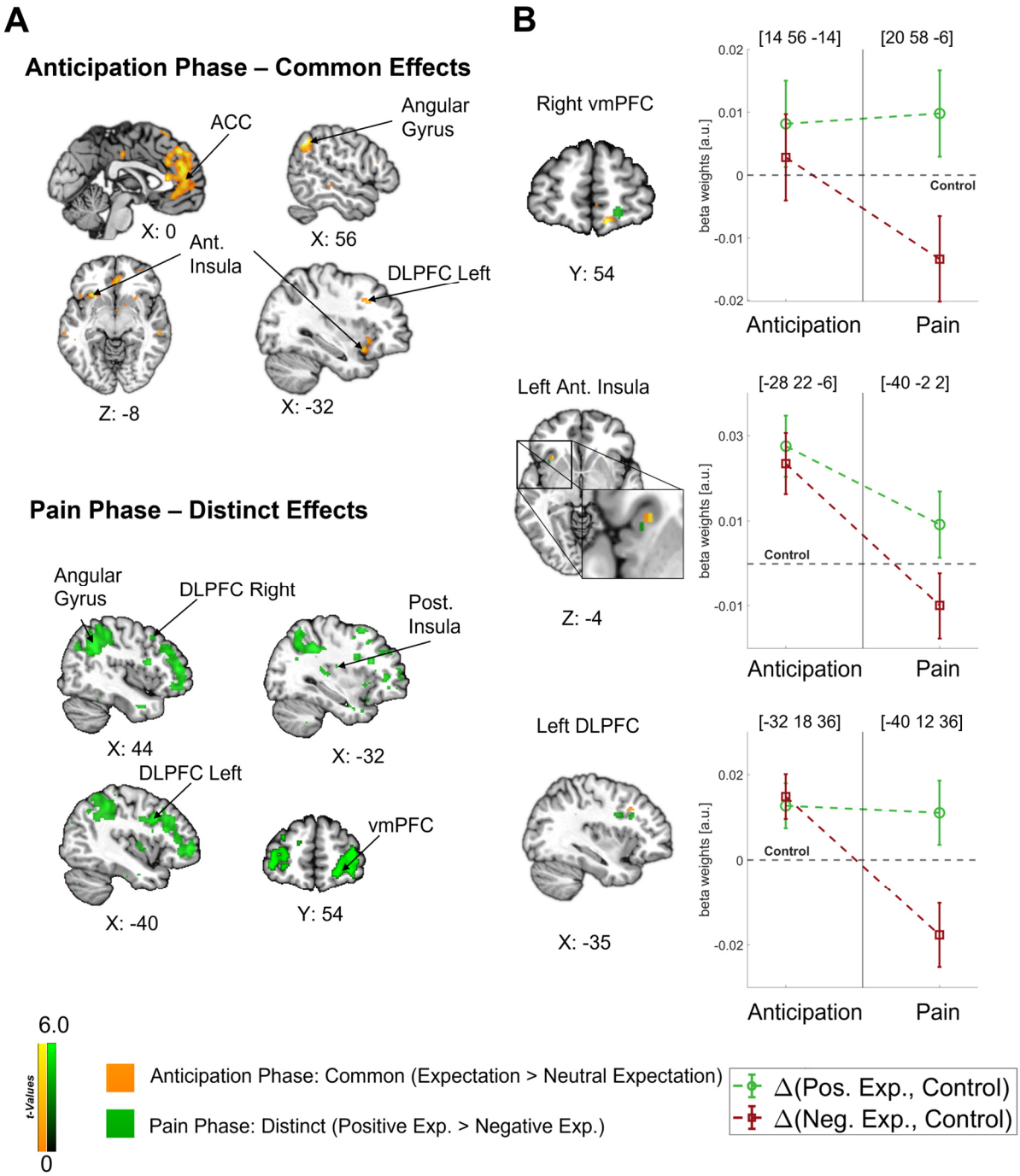

1151

1152 **Differentiation of effects during the anticipation and pain phase.**

1153 **(A) Top:** Common effects during pain anticipation (expectation > neutral expectation)
1154 at $p < .001$ (uncorrected for display purposes) show widespread higher activity for both
1155 positive and negative expectations compared to the control condition. **Bottom:** Distinct
1156 effects (positive > negative) during pain perception are shown, indicating broadly

higher activity for positive compared to negative expectations. **(B) Left**: For selected areas, the overlap between common effects of expectations during the anticipation phase (yellow) and distinct effects of positive and negative expectations during the pain phase (green) in the respective area is shown. **Right**: The corresponding activation levels of positive and negative expectations (i.e., beta weights from the FIR model) baselined by the control condition are plotted for each phase at the respective peaks (peak coordinates in parentheses). The visualization highlights the differentiation of effects following the onset of pain.

1165 **Figure 5**

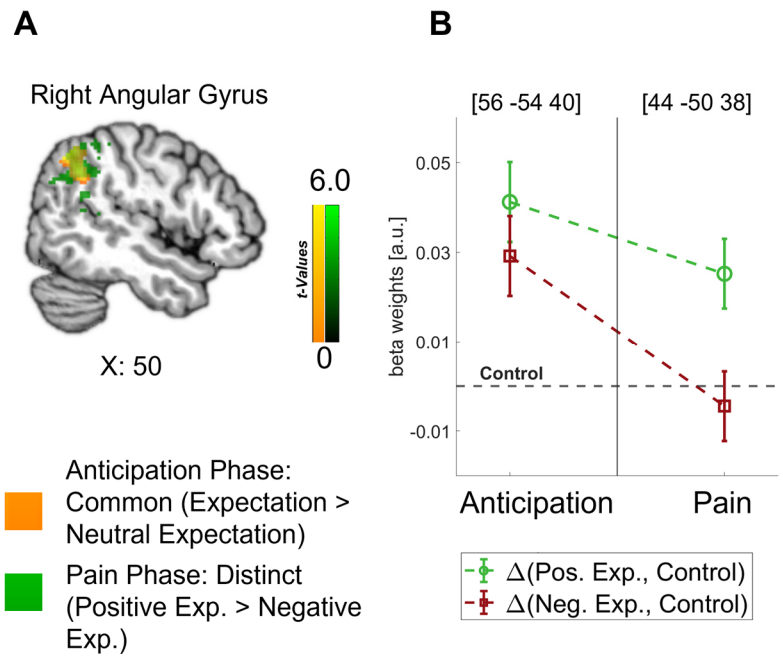

1166

1167 **Representation of Expectations in the Angular Gyrus.**

1168 **(A)** Overlap between common effects of expectations during the anticipation phase
1169 (expectation > neutral expectation; yellow) and distinct effects of positive and negative
1170 expectations during the pain phase (positive > negative; green) is shown for the
1171 angular gyrus at $p < .001$ (uncorrected for display purposes). **(B)** The corresponding
1172 activation levels of positive and negative expectations (i.e., beta weights from the FIR
1173 model) baselined by the control condition are plotted for each phase at the respective
1174 peaks (peak coordinates in parentheses).

1175

1176

1177

1178 **Figure 6**

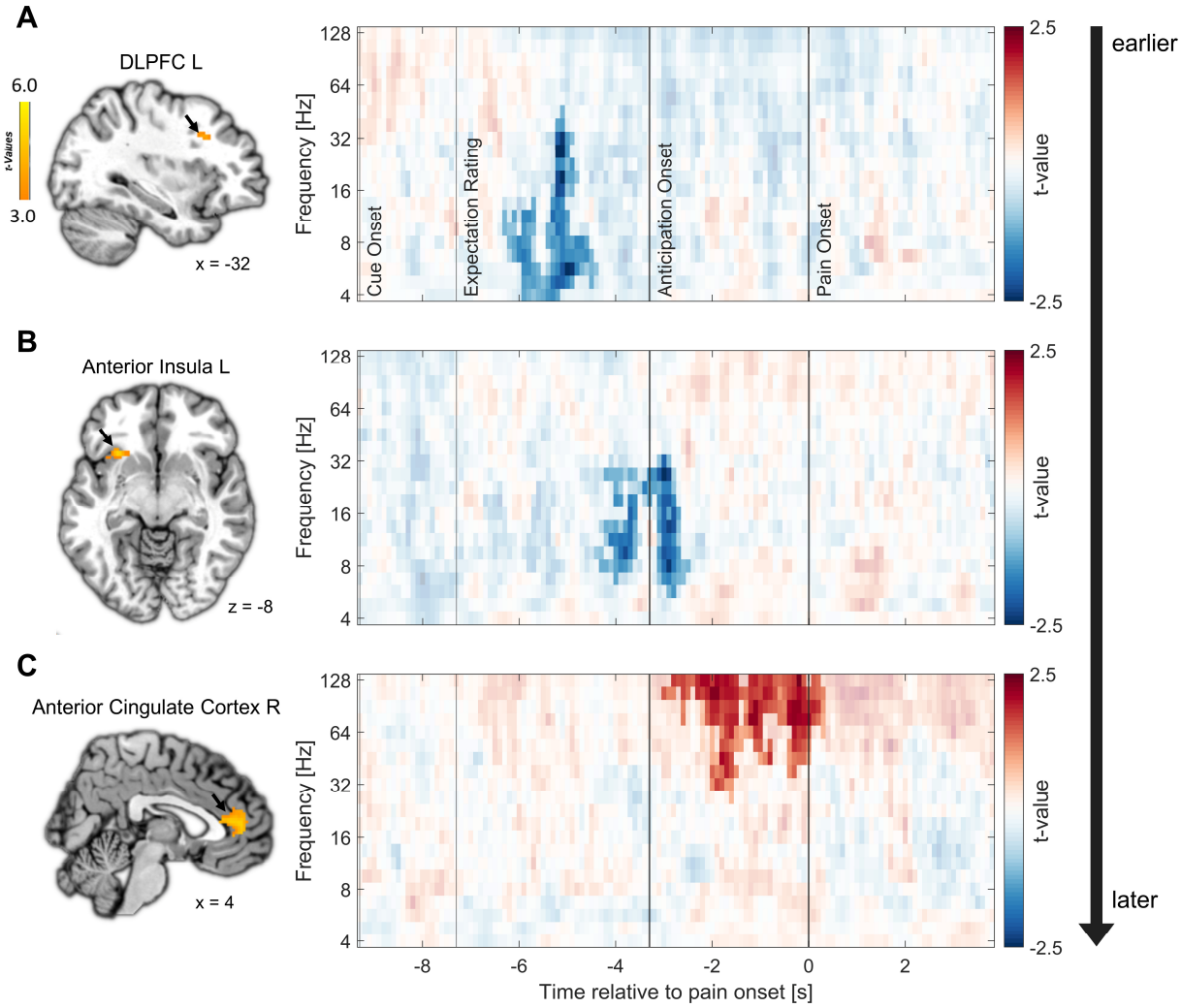

1179

1180 **Relation of fMRI activity with EEG oscillatory power.**

1181 Correlation of single-trial hemodynamic responses with time-frequency resolved EEG
1182 activity in the left DLPFC (A), left anterior insula (B), and right ACC (C) during the
1183 anticipation phase, ordered by the timing of observed correlations as indicated by the
1184 arrow on the right. Single-trial beta weights were extracted from spherical ROIs (10
1185 mm radius) centered around the peak voxels based on the comparison of beta weights
1186 from the FIR model between expectation and neutral expectation during the
1187 anticipation phase, as shown on the left ($p < .001$ uncorrected for display purposes).
1188 On the right, the cluster-corrected correlation of oscillatory power with fMRI activity

averaged over all cluster electrodes is depicted. Non-significant time-frequency points are masked.

10. Tables

Table 1

Characteristics of study participants

	Mean	SD	Range	Number (%)
Gender				
Male				18 (36%)
Female				32 (64%)
Age (years)	25.4	3.5	18 - 34	
FOP				
Severe Pain	36.5	5.4	22 - 47	
Minor Pain	18.9	4.9	10 - 33	
Medical Pain	25.8	6.4	12 - 42	
STADI				
Anxiety	15.2	4.1	10 - 28	
Depression	17.0	3.2	11 - 25	
Global Score	32.2	5.1	23 - 43	
BDI-II Global Score	6.0	3.8	0 - 16	

Note. STADI = State-Trait Anxiety Depression Inventory. FOP = Fear of Pain Questionnaire. BDI-II = Beck Depression Inventory-II.